DE GRUYTER OPEN

DOI: 10.1515/aon-2016-0003

MICHAŁ ŁABOWSKI, PIOTR KANIEWSKI,
PIOTR SERAFIN, BRONISŁAW WAJSZCZYK
Military University of Technology, Warsaw, Poland

OBJECT GEOREFERENCING IN UAV-BASED SAR TERRAIN IMAGES

ABSTRACT

Synthetic aperture radars (SAR) allow to obtain high resolution terrain images comparable with the resolution of optical methods. Radar imaging is independent on the weather conditions and the daylight. The process of analysis of the SAR images consists primarily of identifying of interesting objects. The ability to determine their geographical coordinates can increase usability of the solution from a user point of view. The paper presents a georeferencing method of the radar terrain images. The presented images were obtained from the SAR system installed on board an Unmanned Aerial Vehicle (UAV). The system was developed within a project under acronym WATSAR realized by the Military University of Technology and WB Electronics S.A. The source of the navigation data was an INS/GNSS system integrated by the Kalman filter with a feed-backward correction loop. The paper presents the terrain images obtained during flight tests and results of selected objects georeferencing with an assessment of the accuracy of the method.

Keywords:
georeferencing, synthetic aperture radar, IMU, GNSS.

INTRODUCTION

Georeferencing of objects observed in aerial radar terrain images consists in assigning individual pixels of the image to the ellipsoidal or Cartesian reference frame [Liu and Ozmu, 2009], [Leira et al., 2015]. The georeferencing procedure can be used in modern Battle Management Systems (BMS) to enhance situational awareness of their users. However, the geographical reference of aerial radar

terrain images is a considerable challenge, because their interpretation requires a well-trained technical personnel [Smith, 2012], [Parker, 2012], [Wąż, 2010]. The quality of the radar terrain images is a function of many factors, e.g.: radar sensor parameters (synthetic aperture length, carrier frequency, bandwidth), reflective properties of the objects and in particular the method of collecting the measurement data (a UAV flight trajectory). The radar images are generally not cartographic, they have geometric distortions and the visualizations of the individual objects can be blurred. Moreover interferences and false targets can occur. For these reasons the procedure of interpretation of the radar images is different from the interpretation of the images created using passive sensors operating in the visible range of the electromagnetic spectrum (cameras).

The radar images presented in the article were created using data obtained from the Synthetic Aperture Radar (SAR) [Wang, 2008]. The radar was developed within a project WATSAR carried out by the Military University of Technology and WB Electronics S.A. The paper proposes a method of determining the ellipsoidal coordinates (latitude and longitude) of objects visible on the SAR terrain images. The obtained results were compared with maps which are available at Google Earth environment.

SYSTEM OVERVIEW

The SAR system, which was used in experiments, worked in a Side-Looking Aerial Radar (SLAR) configuration. The Unmanned Aerial Vehicle which carried the Radar Sensor has a wingspan of 5.7 m and a maximum take-off weight of 110 kg. Scanning of the terrain was performed using a StripMap technique. In this method the radar beam should not change its angular position [Wang, 2008]. The geometry of the radar subsystem is shown in Figure 1. For the basic parameters of the radar the reader is referred to the Table 1. In most cases, the StripMap technique assumes that the radar moves along the straight trajectory, at a constants altitude, and with a constant velocity. For systems installed on board a mini-UAV the fulfillment of these requirements is not possible in real world conditions due to the atmospheric air movements. As a consequence, in such systems it is necessary to use techniques which compensate the trajectory disturbances by calculating phase corrections at each point of sending the sounding signal.

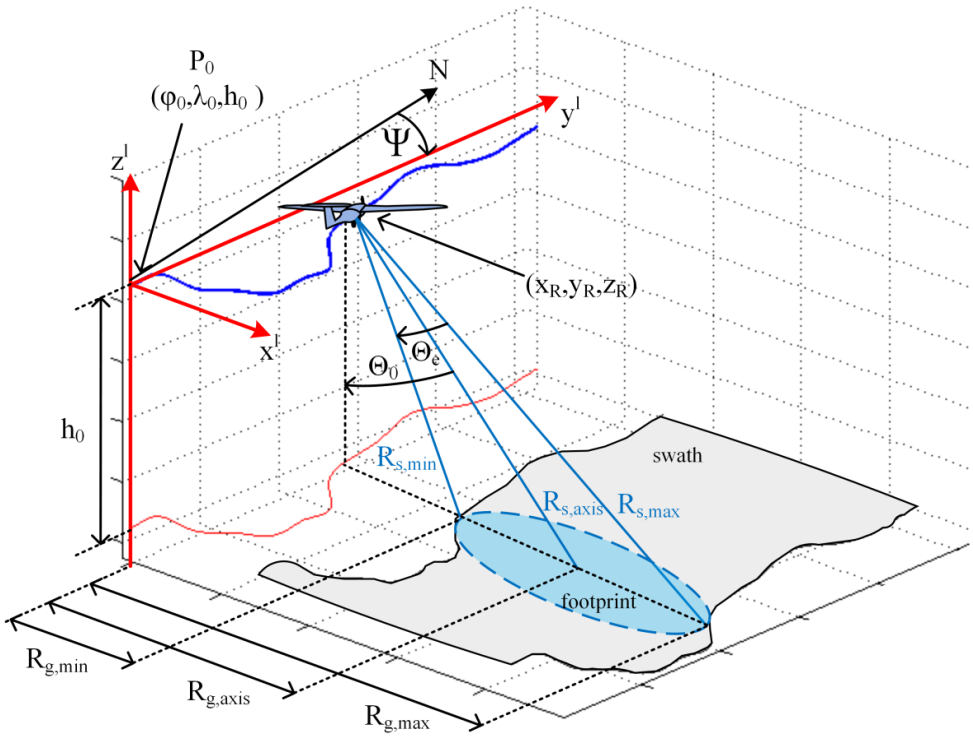

Fig. 1. The radar subsystem geometry: blue line — a real flight path; $P_0 = (\varphi_0, \lambda_0, h_0)$ — *l-frame* origin ellipsoidal coordinates; (x_R, y_R, z_R) — radar coordinates (*l-frame*); $R_{g,min}$, $R_{g,axis}$, $R_{g,max}$ — minimal/antenna axis/maximal ground range; $R_{s,min}$, $R_{s,axis}$, $R_{s,max}$ — minimal/antenna axis/maximal slant range; Θ_e — effective (at the level of –3dB) vertical beamwidth; Θ_0 — antenna incident angle; Ψ — theoretical course of flight

Tab. 1. Main parameters of the Radar Sensor

Parameter name	**Value**	**Unit**
Carrier frequency	15.9	GHz
Bandwidth	180	MHz
Squint angle	0	deg
Antenna –3dB beamwidth in elevation (Θ_e)	30	deg
Antenna incident angle (Θ_0)	45	deg
Pulse Repetition Frequency (PRF)	820	Hz

Some of these methods are based on determination the UAV position in relation to the assumed, theoretical trajectory using navigation systems [Łabowski et al., 2016a], [Samczyński et al., 2014], [Cao et al., 2000], [Gong and Fang, 2007], whereas others calculate the position deviations on the basis of the effects observed in the echo signals (autofocus) [Xing et al., 2009], [Samczyński and Kulpa, 2008].

In WATSAR system the deviations from the assumed flight path are calculated by the INS/GNSS navigation subsystem, in which data integration is realized by the Kalman Filter [Konatowski S. and Pieniężny T., 2007] with feed--backward correction loop. The navigation subsystem consists of: Inertial Measurement Unit (IMU) KVH 1750 with accurate, Fiber Optic Gyros (FOG), dual-antenna GNSS receiver SBG Ekinox-D with active Real Time Kinematic (RTK) option, an embedded Navigation Data Processing Module (NDPM), and a ground, static RTK base station. The navigation subsystem and the method of the navigation correction calculation are described in detail in [Łabowski et al., 2016a], [Łabowski et al., 2016b]. The other components of the WATSAR system are: SAR Processor which calculates the radar image in real time, on board the UAV and the Data Analysis Station which is used to remotely control the on-board elements of the system. A simplified structure of the system is shown in Figure 2. The synchronization of the system components is realized by the synchronization signal generated by the Radar Sensor. The frequency of this signal is equal to the Pulse Repetition Frequency (PRF). The aim of the NDPM is to calculate the navigation correction for the time of each synchronization impulse. Navigation and radar measurement data are also recorded for the purpose of subsequent analysis. The results presented in this paper were obtained in the post processing of the measured data (off-line mode).

The navigation algorithm uses three main reference frames:

- a local, Cartesian reference frame associated with the scanning session (*l-frame*) — it has an origin at the point P_0 which is a location of the radar at the moment of starting of the SAR measurement session (Fig. 1); its Oy^l axis is a theoretical trajectory of flight, the Ox^l axis lies in the horizontal plane and it is directed toward the radar antenna beam, the Oz^l axis points upwards;
- a local, Cartesian, navigation reference frame (*n-frame*) — it has an origin at the point P_0, its axes are geographically orientated toward the north (N), east (E) and local vertical — down (D);
- an Earth-Centered Earth-Fixed frame (*ECEF*) — with a WGS-84 ellipsoid model and ellipsoidal coordinates: φ (latitude), λ (longitude), h (altitude above the ellipsoid).

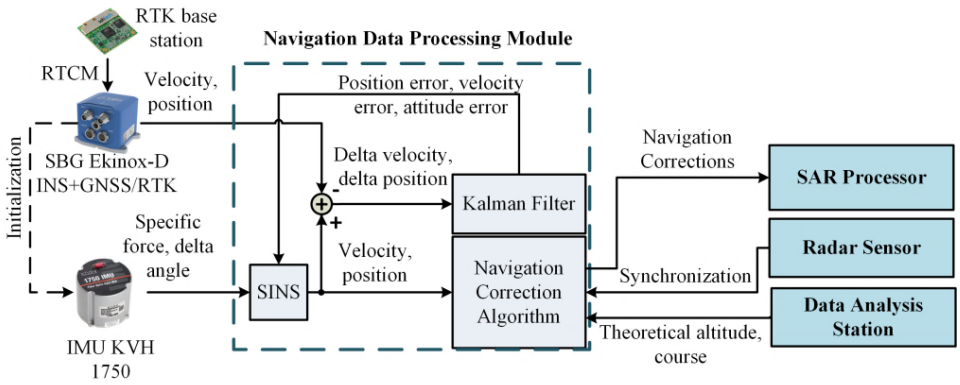

Fig. 2. Simplified structure of the WATSAR system

The components of the navigation corrections are:

- the UAV coordinates expressed in the *l-frame*; each non-zero value of the position measured along the Ox^l and Oz^l axes is a deviation from the presumed, theoretical flight path (Oy^l axis);
- the UAV velocity component measured along the Oy^l axis.

The application of the navigation corrections within the echo signals phase correction procedure reduces the geometric distortions of the image. Moreover, it improves the distinguishability of individual targets by reduction of the blurring effect [Łabowski et al., 2016a].

GEOREFERENCING TECHNIQUE

The aim of the presented georeferencing method is to determine the ellipsoidal coordinates of objects selected by the user, who analyzes the radar terrain image. The indication of the objects takes place in a dedicated PC application via a mouse click at the desired location on the image. The georeferencing algorithm is based on navigation corrections which are used to improve the quality of the SAR image.

In the presented scenario, the georeferencing steps are as follows:

1) loading of the measurement data (radar and navigation);
2) navigation corrections computation;
3) SAR image calculation;

4) radar terrain image analysis by the user;
5) selection of the image point (pixel) whose coordinates have to be computed;
6) calculation of the object coordinates, expressed in the *l-frame*;
7) conversion of the object coordinates, from the *l-frame* to the *n-frame*;
8) conversion of the object coordinates, from the *n-frame* to the *ECEF* (latitude and longitude).

The radar terrain images are obtained as a result of the SAR image synthesis process. The individual pixels, which belong to the same single line of the image (in range direction) can be expressed in a fast time domain. The fast time τ is a time of arrival of the echo signal reflected from the terrain object (Fig. 3). The fast time domain is proportional to a slant range domain, where the slant range is the distance between the radar and the object. The slant range R_{s1} to the object No. 1 in Figure 3, is given by the equation:

$$R_{s1} = c\tau_1, \tag{1}$$

where:

c — speed of light,

τ_1 — the fast time associated with the echo signal from object No. 1.

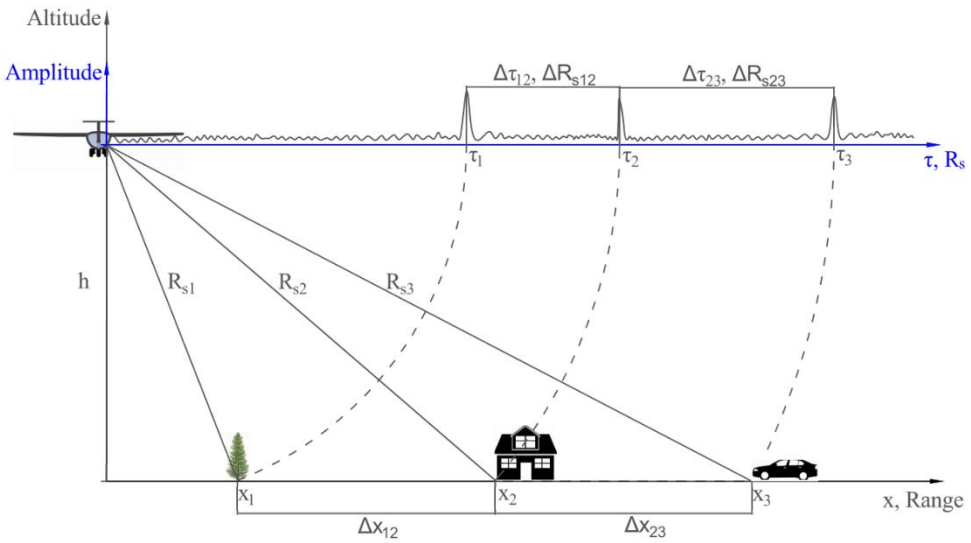

Fig. 3. Slant and ground ranges between the radar and the objects

Ground range describes the distance between the radar and the object, measured in the horizontal plane. In the simplified case shown in Figure 3 the distances between ground ranges to objects No. 1, 2 and 3, are equal:

$$\Delta x_{12} = \Delta x_{23}. \tag{2}$$

However, due to the geometry of the radar subsystem, the distances between the slant ranges to objects No. 1, 2 and 3, are not equal:

$$\Delta R_{s12} \neq \Delta R_{s23}.$$

The x^l coordinate of the chosen pixel, expressed in the *l-frame*, can be calculated using the following formula:

$$x^l(k) = \sqrt{(k \cdot dR)^2 - h^2}\ , \tag{3}$$

where:

k — number of the pixel in a line of the image (range direction),
h — altitude of flight above the ground level,
$x^l(k)$ — ground range to the object,
dR — size of the range cell [Wang, 2008].

Determination of the object y^l coordinate is based on navigation corrections. The corrections are calculated for the each radar measurement. Each line of the image (in range direction) is a result of synthesis of the aperture which has a predetermined length (number of soundings). Assuming that the chosen pixel is located in a line, which was calculated on the basis of the radar measurements numbered in range $<m_1, m_2>$, the resulting y^l coordinate of the pixel equals to the y^l coordinate of the radar position associated with the center of the synthetic aperture — m_p (Fig. 4):

$$m_p = \frac{1}{2}(m_1 + m_2). \tag{4}$$

Conversion of the object coordinates, from the *l-frame* to the *n-frame*, is realized using the following equations:

$$N = x^l \cdot \cos\left(\Psi + \frac{\pi}{2}\right) + y^l \cdot \sin\left(\Psi + \frac{\pi}{2}\right); \tag{5}$$

$$E = x^l \cdot \sin\left(\Psi + \frac{\pi}{2}\right) - y^l \cdot \cos\left(\Psi + \frac{\pi}{2}\right), \tag{6}$$

where:

N, E — north/east coordinate of the object position,

Ψ — an angle between the Oy^l axis and geographic north direction (course).

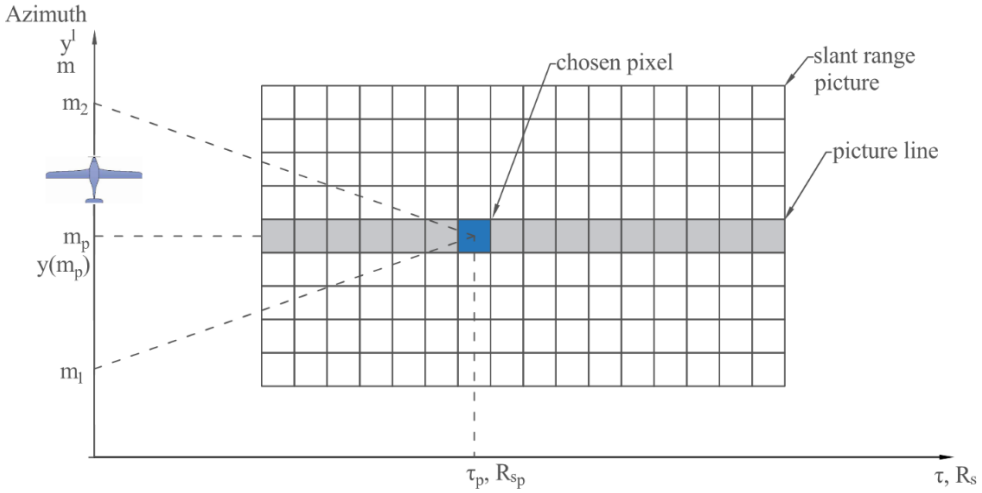

Fig. 4. Principle of calculation of the y^l coordinate: m — number of the radar measurement; m_1, m_p, m_2 — number of the radar measurement at the beginning/middle/end of the aperture associated with chosen pixel

The last step of the georeferencing method is to determine the latitude and longitude of the selected object, according to the formulae:

$$\varphi = \varphi_0 + \frac{N}{R_N + h_{wgs}}; \tag{7}$$

$$\lambda = \lambda_0 + \frac{E}{\left(R_E + h_{wgs}\right) \cdot \cos\varphi}, \tag{8}$$

where:

φ, λ — latitude and longitude of the selected object,

R_N, R_E — meridian and transverse radiuses of curvature of the WGS-84 ellipsoid,

h_{wgs} — altitude above the WGS-84 ellipsoid.

RESULTS

The georeferencing technique has been verified using measurement data recorded during the flight, whose trajectory is shown in Figure 5. The flight was performed on July 9th, 2015 in Kamień Śląski airfield. A green polygon in Figure 5 is a theoretically derived region scanned by the Radar Sensor (swath) — its boundaries were calculated using an antenna beamwidth in the range direction (at –3dB level), and 45º antenna incident angle. Orange line is the presumed, theoretical flight path (Oy^l axis), whereas a red line is the real flight path obtained from the INS/GNSS navigation system. The altitude of flight (above the ground level) was approximately 150 m. A SAR terrain image, obtained by post-processing of stored data (the length of synthetic aperture equals 200 measurements), is shown in Figure 6. The radar image was created with a use of the navigation corrections.

Fig. 5. UAV real and theoretical flight trajectory
[used application Google Earth]

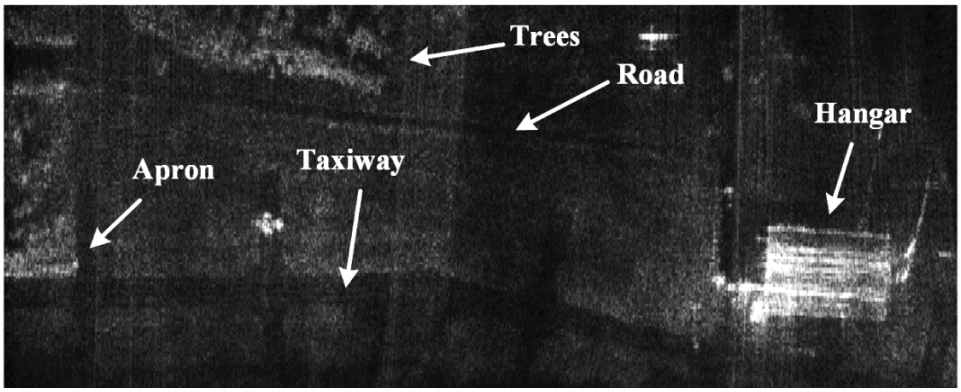

Fig. 6. SAR radar terrain image

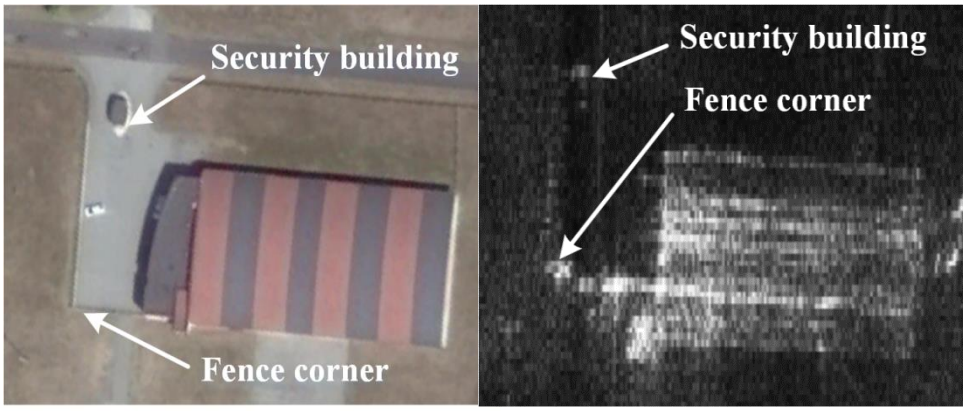

Fig. 7. Georeferenced objects: an aerial photo (left) and radar image (right)

Fig. 8. Results of the georeference (red markers – Google Earth, white markers – SAR) [used application Google Earth]

Table 2 shows the differences in object coordinates obtained from the Google Earth and the georeferencing procedure.

Tab. 2. Object coordinates comparison

Object	Coordinates (Google Earth)	Coordinates (georeferencing)	Difference
Security building	50°31'52.12"N	50°31'51.80"N	9,88 m
	18° 5'36.79"E	18° 5'36.70"E	1,77 m
Fence corner	50°31'51.08"N	50°31'50.90"N	5,56 m
	18° 5'35.73"E	18° 5'35.70"E	0,59 m

Reasons of the differences in coordinates are as follows:

- in case of large objects (e.g. security building) it is difficult to choose exactly the same part (or pixel) of it in the optical photo and the radar image;
- range resolution of used Radar Sensor is worse than azimuth resolution (0.5 m achievable), which increases the error associated with the x^l coordinate; as a result in many cases it is impossible to distinguish the details of the object;
- potential application of the Hanning weighting window can degenerate the range resolution to about 1.5 m, but allows to reduce the range side lobes level (the range resolution of the original image is about 0.8 m);
- foreshortening and layover — geometrical distortions of high objects in SAR images, resulting from the projection onto ground range plane; as a result, in case of a steep slope the top of the object can cover its base (layover) or if the slope is gentle, the top can be displaced toward the near range compared to its actual map position, and the object appears to be leaning toward the Radar Sensor (foreshortening) [Smith, 2012].

CONCLUSIONS

The paper presents the method of determining the ellipsoidal coordinates of the objects observed in the radar terrain images. During the test campaign the measurement system was installed on board a mini UAV. Presented results were obtained during post-processing of data recorded during the flight. From the perspective of the georeferencing procedure a key component of the measurement system is its navigation part. The aim of the navigation subsystem is to make

measurements using IMU and GNSS receiver. The obtained data allow to determine the UAV position displacements in relation to the rectilinear trajectory of flight, which is required by the adopted method of SAR measurements. Navigational corrections are used to improve the quality of the radar images (to reduce the geometric distortions), and are necessary for the georeferencing procedure. Navigation data allow for direct determination of the azimuthal coordinate (y^l) of the selected image line. Moreover, they are used in calculation of the range coordinate (x^l) by measuring the altitude above the reference ellipsoid. The navigation subsystem also provides data necessary to convert the radar coordinates from the local reference system (*l-frame*) to the *ECEF* (latitude and longitude).

Thanks to the GNSS receiver with RTK option, and the IMU with precise FOG gyros, it is possible to accurately determine the position of the UAV during the flight (the position error in horizontal plane is lower the 0.1 m). A class of the navigation subsystem has a significant impact on the accuracy of the final results of the georeferencing procedure. However, the accuracy is degraded due to the natural properties and processes associated with the SAR technique, e.g.: weighting windows, foreshortening and layover phenomena. Improvement of the range resolution can be achieved by increasing the bandwidth of the radar signal — currently in Radar Sensor form WATSAR system it equals 180 MHz. The precise estimation of the position error caused by the georeferencing procedure requires an analysis of more measurement situations. In obtained results this error was less than 10 m, which is acceptable in many applications, such as modern Battle Management Systems or Search And Rescue missions.

REFERENCES

[1] Cao F., Bao Z., Yuan J., Motion compensation for aerial SAR, 5th International Conference on Signal Processing Proceedings, Beijing 2000, pp. 1864–1867.

[2] Gong X., Fang J., Analyses and comparisons of some nonlinear Kalman Filters in POS for airborne SAR motion compensation, International Conference on Mechatronics and Automation ICMA, 2007, pp. 1495–1500.

[3] Konatowski S., Pieniężny T., A comparison of estimation accuracy by the use of KF, EKF and UKF filters, Computational Methods and Experimental Measurements CMEM, WIT Press Southampton, 2007, pp. 779–789.

[4] Leria F., Trnka K., Fossen T., Johansen T., A light-Weight Thermal Camera Payload with Georeferencing Capabilities for Small Fixed-Wing UAVs, International Conference on Unmanned Aircraft System, 2015, pp. 485–494.

[5] Liu L., Ozmu M., Encyclopedia of Database Systems, Springer, 2009.

[6] Łabowski M., Kaniewski P., Serafin P., Inertial navigation system for radar terrain imaging, 2016 IEEE/ION Position, Location and Navigation Symposium (PLANS), Savannah, GA, 2016, pp. 942–948.

[7] Łabowski M., Kaniewski P., Konatowski S., Estimation of Flight Path Deviations for SAR Radar Installed on UAV, 'Metrology and Measurement Systems', 2016, Vol. 23, Issue 3, pp. 383–391.

[8] Parker W., Discover the Benefits of Radar Imaging, 'EJE Earth Imaging Journal', 2012.

[9] Samczynski P., Kulpa K., Non iterative map-drift technique, International Conference on Radar, 2008, pp. 76–81.

[10] Samczynski P., Malanowski M., Gromek D., Gromek A., Kulpa K., Krzonkalla J., Mordzonek M., Nowakowski N., Effective SAR image creation using low cost INS/GPS, 15th International Radar Symposium (IRS), 2014, pp. 1–4.

[11] Smith R., Introduction to Interpreting Digital Radar Images with TNTmips, Micro-Images Inc., 2012.

[12] Wang B., Digital signal processing techniques and applications in radar image processing, John Willey & Sons, New Jersey 2008, pp. 155–160.

[13] Wąż M., Problems with precise matching radar image to the nautical chart, 'Annual of Navigation', 2010, No. 16, pp. 149–164.

[14] Xing M., Jiang X., Wu R., Zhou F., Bao Z., Motion compensation for UAV SAR based on raw radar data, 'IEEE Transactions on Geoscience and Remote Sensing', 2009, Vol. 47, No. 8, pp. 2870–2883.

Received September 2016
Reviewed November 2016

MICHAŁ ŁABOWSKI
Military University of Technology
Kaliskiego 2 Str., 201-476 Warsaw, Poland
e-mail: michal.labowski@wat.edu.pl

PIOTR KANIEWSKI
Military University of Technology
Kaliskiego 2 Str., 201-476 Warsaw, Poland
e-mail: piotr.kaniewski@wat.edu.pl

PIOTR SERAFIN
Military University of Technology
Kaliskiego 2 Str., 201-476 Warsaw, Poland
e-mail: piotr.serafin@wat.edu.pl

BRONISŁAW WAJSZCZYK
Military University of Technology
Kaliskiego 2 Str., 201-476 Warsaw, Poland
e-mail: bronislaw.wajszczyk@wat.edu.pl

STRESZCZENIE

Lotnicze zobrazowania terenu realizowane za pomocą radaru z syntetyczną aperturą pozwalają na uzyskanie wysokiej rozróżnialności porównywalnej z rozróżnialnością metod optycznych, mając jednocześnie nad nimi przewagę w postaci niezależności obserwacji od warunków pogodowych czy pory dnia. Proces analizy tak uzyskanych zobrazowań składa się przede wszystkim z identyfikacji interesujących obiektów. Możliwość określenia ich współrzędnych geograficznych pozwala na znaczące zwiększenie użyteczności tego rozwiązania z punktu widzenia potencjalnego użytkownika. W artykule przedstawiono metodę georeferencji zobrazowań terenu otrzymywanych za pomocą radaru z syntetyczną aperturą, który zainstalowano na pokładzie bezzałogowego statku powietrznego. System taki opracowano w ramach projektu WATSAR, zrealizowanego przez Wojskową Akademię Techniczną i WB Electronics S.A. Źródłem danych nawigacyjnych był system INS/GNSS, zintegrowany metodą filtracji pośredniej, z korekcją wstecz. W artykule zamieszczono radarowe zobrazowania terenu uzyskane podczas badań poligonowych systemu oraz wyniki georeferencji wybranych obiektów wraz z oceną dokładności wyznaczanego położenia.